

## X-ray photoemission spectroscopy as a probe of charge-gap opening in many-electron systems

This article has been downloaded from IOPscience. Please scroll down to see the full text article.

2001 J. Phys.: Condens. Matter 13 10089

(<http://iopscience.iop.org/0953-8984/13/44/320>)

View [the table of contents for this issue](#), or go to the [journal homepage](#) for more

Download details:

IP Address: 171.66.16.226

The article was downloaded on 16/05/2010 at 15:06

Please note that [terms and conditions apply](#).

# X-ray photoemission spectroscopy as a probe of charge-gap opening in many-electron systems

Robert Haslinger<sup>1</sup> and Nic Shannon<sup>2</sup>

<sup>1</sup> Department of Physics, UW–Madison, Madison, WI-53706, USA

<sup>2</sup> Max-Planck-Institut für Physik komplexer Systeme, Nöthnitzer Strasse 38, 01187 Dresden, Germany

Received 24 July 2001

Published 19 October 2001

Online at [stacks.iop.org/JPhysCM/13/10089](http://stacks.iop.org/JPhysCM/13/10089)

## Abstract

Core-hole (x-ray) photoemission (XPS) provides a powerful indirect probe of the low-energy charge excitations of a many-electron system. We have previously argued that XPS can be used to study the way in which a (pseudo)gap opens for charge excitations across, for example, a metal–superconductor transition, *independently* of any change in the spin excitation spectrum, and so provide information about spin–charge separation. Here we consider how the loss of low-energy excitations modifies XPS spectra in the context of several simple models, considering particularly the case of gap opening for both s- and d-wave superconductors, and find that XPS, like the nuclear magnetic resonance technique, is in principle sensitive to nodes in the superconducting gap function.

## 1. Introduction

As a many-electron system undergoes a phase transition, the nature of its low-energy excitations is usually radically altered. For this reason, experiments which are sensitive to the rearrangement, and in particular to the loss of, low-energy excitations (to the opening of a gap) can inform us about how phase transitions take place. Nuclear magnetic resonance (NMR) has been used widely in this context to study how low-lying *spin* excitations evolve in different phases. Famously, NMR reveals a second ‘transition’ temperature  $T^*$  in the underdoped cuprate superconductors, below which a gap opens for spin (and probably charge) excitations, even in the absence of superconducting order [1].

One of us has proposed the use of core-level (x-ray) photoemission (XPS) as a probe complementary to NMR, offering similar insight into the evolution of *charge*-carrying excitations [2,3]. The opening of a charge gap in a metallic system has certain simple systematic consequences for XPS lineshapes—an overall shift in the core line to higher binding energy, and a transfer of spectral weight from high energies to the line threshold. These effects are both due to the suppression of low-energy charge-density fluctuations and can be understood on quite general physical grounds without recourse to specific models or calculations. Most

importantly, such modifications of the XPS lineshape depend only on variations in the *charge* spectrum near the Fermi surface. Within the usual picture by means of which XPS spectra are understood, similar variations in the spin spectrum have *no* effect on XPS lineshapes.

The ability to probe the spin and charge spectra *separately* would be extremely useful for exploring potential *spin-charge-separated* systems. It has been suggested by some that the NMR-observed pseudogap at  $T^*$  in the underdoped cuprates is actually a spin gap. This proposal is, of course, hotly contested, but the application of separate spin (NMR) and charge (XPS) probes could help resolve the issue, and evidence for a (pseudo)gap opening for charge excitations at  $T^*$  has been inferred from the temperature dependence of XPS spectra [16]. There are many other scenarios in which such a comparison might also be useful—for example in metal–insulator transitions where electron–electron interaction is strong, or in one-dimensional materials for which theory, for example the Luttinger–Tomonaga models, often suggests spin–charge separation.

In this article we extend the analysis of [2, 3] to try to understand the most general consequences of charge-gap opening for XPS—the systematic changes which can be expected to occur in the simplest observed lineshapes—for simple models, in a quantitative way. A good understanding of the behaviour of the simplest models is clearly a necessary first step before attempting the more complicated task of interpreting real experimental data from complicated materials such as the cuprates or 1D charge-density-wave systems. With this in mind we make a detailed case study of the way in which the familiar asymmetric Doniach–Sunjic lineshape for a core level in a metal [4] is modified by a phase transition to a gapped semiconductor or superconductor.

We begin in section 2 with a review of the simple perturbative formalism used to calculate XPS lineshapes and associated shifts. In section 3 we calculate the XPS spectrum for a band metal and a simple toy model of a semiconductor within perturbation theory. In section 4 we consider lineshapes and shifts of s- and d-wave superconductors for a free-electron gas and a d-wave superconductor on a two-dimensional tight-binding lattice at half-filling.

In the concluding section, section 6, we discuss the consequences and limitations of these results, as applied to experiment, making a comparison with angle-resolved photoemission (ARPES) and emphasizing the potential role of XPS as a diagnostic tool for strongly correlated systems.

## 2. Formalism

In an XPS experiment a high-energy (x-ray) photon ejects a single electron from a tightly bound atomic level in the sample material, typically a prepared metal surface. The energy distribution of the emitted photoelectrons is measured. Within the sudden approximation, and neglecting all momentum dependence of the matrix elements, the XPS lineshape for the core level is simply proportional to the spectral function for the resulting core hole [5]. Because photoemission leaves behind this unscreened and massive positive charge (recoil of the core hole can safely be neglected) it is accompanied by a violent low-energy ‘shake-up’ of the remaining itinerant electrons. This many-body effect has important consequences for the core lineshape, as described below, and it is the suppression of the ‘shake-up’ by a gap for charge excitations which makes XPS useful as a probe of different phases.

In practice various other mechanisms serve to limit the lifetime of the core hole—which must eventually be filled by the decay of an electron from a higher energy level—and we model these by convoluting the calculated lineshape with a Lorentzian whose width is the inverse core-level lifetime. We neglect a further (temperature-dependent) broadening due to phonon processes, which could be accounted for by further convolution with a Gaussian.

Perhaps more importantly, we do not consider either the possibility of single atomic lines being split into multiplets by interaction with neighbouring atoms on the lattice (which is important for some core levels in the cuprates [6]), or the case in which the core hole binds an itinerant electron. The latter can also lead to multiple lines accompanying each core level, and has been treated for the ordinary free-electron gas by several authors [7].

We model the combined system of core-level and itinerant electrons with the simple Hamiltonian

$$\mathcal{H} = \mathcal{H}_0 + \mathcal{V}_c \quad (1)$$

where  $\mathcal{H}_0$  is the unperturbed Hamiltonian describing the itinerant-electron system, and

$$\mathcal{V}_c = \epsilon_d d^\dagger d + V(t) = \epsilon_d d^\dagger d + \frac{1}{v^2} \sum_{k,q} V(q) c_{k-q}^\dagger(t) c_k(t) \quad (2)$$

is switched on suddenly at  $t = 0$  when the core hole is created.  $\epsilon_d$  is the energy of the core hole,  $d$  is the core-hole annihilation operator, and  $c$  is the electron annihilation operator. Spin does not enter into the problem and has been suppressed in our notation.

We model the gapless system as a band of spinless non-interacting electrons

$$\mathcal{H}_0 = \sum_k \epsilon_k c_k^\dagger c_k \quad (3)$$

characterized by a density of states  $N(\omega) = \sum_k \delta(\omega - \epsilon_k)$ . Semiconductors are modelled in the same way, but with zero density of states within the gap  $|\omega| < \Delta$ . We use the usual BCS (Bardeen–Cooper–Schrieffer) description of superconducting systems, with quasiparticle dispersion  $E_k^2 = \epsilon_k^2 + \Delta_k^2$ , where  $\epsilon_k$  is the underlying band dispersion and  $\Delta_k$  the (momentum-dependent) superconducting order parameter.

Within the sudden approximation [5], the XPS spectrum is proportional to the core-electron spectral function

$$A_h(\omega) = -2 \text{Im}\{G_h^{ret}(\omega)\} \quad (4)$$

where  $G_h^{ret}(\omega)$  is the retarded core-hole Green's function. From this definition it follows that the spectral function is normalized to  $2\pi$ , and spectral weight must always be conserved in XPS lineshapes.

The Green's function for the core hole must be calculated using the full wavefunction for the many-electron system *including* the itinerant electrons, and therefore involves matrix elements for the overlap of the many-electron ground state with all the different states excited by the suddenly switched core hole. In this indirect way XPS probes the spectrum of the itinerant-electron liquid.

In the absence of any interaction with the core hole ( $V(q) \equiv 0$ ) the itinerant electrons remain in their ground state and the core-hole spectral function is a single coherent delta-function peak

$$A_h(\omega) = 2\pi \delta(\omega - \epsilon_d). \quad (5)$$

Interaction with itinerant electrons transfers spectral weight to an incoherent tail and, under certain conditions, eliminates the coherent (delta-function) part of the spectral function entirely.

We evaluate  $G_h^{ret}(t)$  in the presence of interaction ( $V(q) \neq 0$ ) using a linked-cluster expansion [8]

$$G_h^{ret}(t) = -i\theta(t)e^{-i\epsilon_d t} \exp \left[ \sum_{l=1}^{\infty} F_l(t) \right] \quad (6)$$

where the coefficients  $F_l(t)$  are given by

$$F_l(t) = \frac{1}{l}(-i)^l \int_0^t dt_1 \cdots \int_0^t dt_l \langle |TV(t_1) \cdots V(t_l)| \rangle_{\text{connected}}. \quad (7)$$

The leading term in this series,  $F_1(t)$ , is purely real and contributes only an absolute shift in the core line. For a purely local interaction ( $V(q) = V_0$ ), this is simply proportional to the density of electrons, and therefore unchanged by the opening of a gap.

It is the second-order term,  $F_2(t)$ , which contains interesting many-body physics and, to second order in  $V(q)$ , determines the XPS lineshape. This is seen to be related to the density–density correlation function (charge susceptibility), and indeed it can be rewritten as

$$F_2(t) = \frac{1}{v} \sum_q |V(q)|^2 \left\{ \frac{i}{2} \chi'_\rho(q, \omega = 0)t + \frac{1}{\pi} \int_0^\infty d\omega \chi''_\rho(q, \omega) \frac{1 - e^{-i\omega t}}{\omega^2} \right\} \quad (8)$$

where  $\chi'_\rho$  and  $\chi''_\rho$  are the real and imaginary parts of the retarded density–density correlation function in frequency space [9].

The first part of this expression is an energy shift. It is sensitive to the opening of a gap and for delta-function interaction it is proportional to the real part of the local charge susceptibility. The second, more complicated term, determines the lineshape. We write this as

$$\bar{F}_2(t) = - \int_0^\infty d\omega R(\omega) \frac{1 - e^{-i\omega t}}{\omega^2} \quad (9)$$

where

$$R(\omega) = -\frac{1}{\pi} \sum_q |V(q)|^2 \chi''_\rho(q, \omega) \quad (10)$$

is a spectral representation of the perturbation. The core-hole–itinerant-electron interaction  $V(q)$  is short ranged, and for the purposes of this article may be approximated by the purely local interaction  $V(q) = V_0$ , so

$$R(\omega) = -\frac{1}{\pi} |V_0|^2 \sum_q \chi''_\rho(q, \omega). \quad (11)$$

To find the XPS lineshape within these approximations is then a matter of calculating the imaginary part of the local density–density correlation function as a function of frequency. In the next section we work through several examples, rederiving the familiar asymmetric (Doniach–Sunjic) lineshape for a core level in a metal and showing how it is modified by the opening of a gap in the excitation spectrum.

### 3. Band metals and semiconductors

In this section we will calculate the lineshape for a normal metal, modelled as a band of non-interacting electrons using equation (9), and observe how it changes when a gap is opened in the density of states. For simplicity we assume zero temperature and a delta-function potential for the core hole.

Within a non-interacting picture,  $R(\omega)$  can be found from the imaginary part of the particle–hole bubble:

$$R(\omega) = \frac{|V_0|^2}{v^2} \sum_{k,p} [n(\xi_p) - n(\xi_k)] \delta(\omega + \xi_p - \xi_k). \quad (12)$$

We consider a flat density of states centred about the Fermi energy, such that

$$N(\omega) = \begin{cases} N_0 & |\omega| < \epsilon \\ 0 & |\omega| > \epsilon. \end{cases} \quad (13)$$

$R(\omega)$  is then easily calculated:

$$R(\omega) = \begin{cases} \alpha\omega & 0 < \omega < \epsilon \\ \alpha(2\epsilon - \omega) & \epsilon < \omega < 2\epsilon \\ 0 & \omega > 2\epsilon \end{cases} \quad (14)$$

where  $\alpha = 2N_0^2|V_0|^2$  (the 2 is from the spin summation). In what follows we will use  $\alpha$  as a parameter, rather than separately specifying the bare density of states  $N_0$  and the interaction strength  $V_0$ . Since these are unchanged by the opening of a gap, values of  $\alpha$  found from experiments on the metallic phase of materials can be used to parametrize predictions for the their XPS lineshapes in a gapped phase. Empirically,  $\alpha \sim 0.1$  for most simple metals, and all plots in this paper have been calculated for  $\alpha = 0.1$ .

On substitution of equation (14) in equation (9) we find that the expected delta function at threshold is lost and instead  $A(\omega)$  diverges as  $\omega^{\alpha-1}$  as  $\omega \rightarrow 0_+$ . This power-law singularity is broadened by the core-hole lifetime, yielding an asymmetric lineshape essentially equivalent to that calculated by Doniach and Sunjic [4]. The XPS lineshape for this simple band metal formed by numerically convoluting the spectral function with a Lorentzian lifetime envelope is plotted in figure 1. We have reversed the energy axis in this and all other plots of lineshapes for ease of comparison with photoemission spectra.

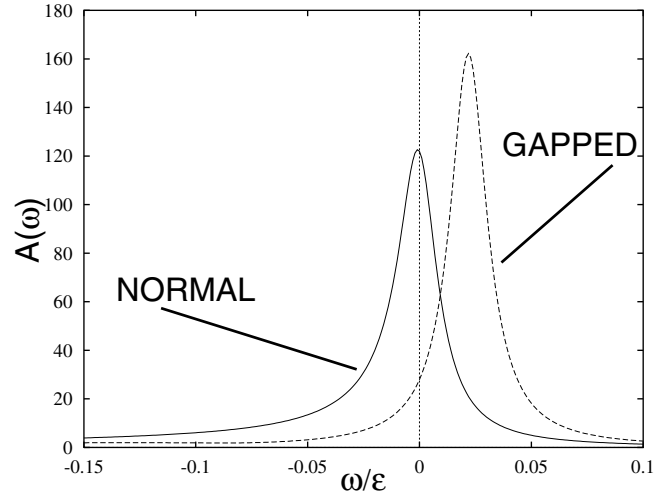


**Figure 1.** XPS lineshapes for the flat-density-of-states model with and without a gap of  $\Delta/\epsilon = 0.05$ . The inverse core-hole lifetime is  $1/\tau = 0.01\epsilon$ , and  $\alpha = 0.1$ . The opening of a gap causes spectral weight to be shifted out of the power-law tail and back into the restored delta-function peak. In addition, the entire XPS lineshape (delta function and incoherent tail) undergoes a rigid shift to lower binding energy.

The replacement of the delta-function peak in  $A_h(\omega)$  with a power-law singularity is a consequence of Anderson's *orthogonality catastrophe* [10, 11]. The sudden switching of the core hole in the photoemission process leads to the creation of itinerant-electron-hole pairs with all possible energies and therefore to a high-energy tail in the spectral function. Since the

number of electron–hole pairs created with zero energy is logarithmically divergent, the ground states of the perturbed and unperturbed systems are orthogonal, and there is no delta-function peak at threshold. The orthogonality catastrophe is effective in a band of non-interacting electrons whenever the density of states at the chemical potential is finite, i.e. for any band metal. While all our analysis is limited to second order in the potential  $\mathcal{V}$ , this is usually small, and the physics of the orthogonality catastrophe is in any case essentially unaltered by the inclusion of higher-order processes (multiple particle–hole excitations) [13].

We now calculate the lineshape for a toy model of a gapped system. The presence of the gap will cut off the number of low-energy excitations made by the core hole, eliminating the orthogonality catastrophe. The gap has little effect at higher energies, so away from threshold the lineshape for a system with a small gap should be essentially unchanged. The failure of the orthogonality catastrophe will however lead to the restoration of a delta-function peak at threshold. As the gap becomes bigger, progressively more spectral weight is transferred to this peak, so for large gaps the effective lineshape after convolution with a Lorentzian will be the symmetric peak associated with an insulator.

At the same time the overall threshold for the XPS line is shifted to lower energies because the redistribution of charge in the electron gas is suppressed by the opening of the gap, and therefore less work is done inserting a core hole into the system.

If, for the sake of illustration, we assume that a gap opens such that the new density of states is

$$N(\omega) = \begin{cases} N_0 \left( \frac{\epsilon}{\epsilon - \Delta} \right) & -\epsilon < \omega < -\Delta \\ N_0 \left( \frac{\epsilon}{\epsilon - \Delta} \right) & \Delta < \omega < \epsilon \\ 0 & \text{otherwise} \end{cases} \quad (15)$$

then  $R(\omega)$  is modified in a straightforward way:

$$R(\omega) = \begin{cases} 0 & \omega < 2\Delta \\ \tilde{\alpha}(\omega - 2\Delta) & 2\Delta < \omega < \epsilon + \Delta \\ \tilde{\alpha}(2\epsilon - \omega) & \epsilon + \Delta < \omega < 2\epsilon \end{cases} \quad (16)$$

where  $\tilde{\alpha} = (\epsilon/\epsilon - \Delta)^2 \alpha$  (figure 2). This new form of  $R(\omega)$  (the imaginary part of the charge susceptibility) completely determines the revised lineshape through equation (9).

On the other hand it is the change in the real susceptibility which leads to the shift in the XPS line. The real and imaginary parts of the density correlation function are connected via Kramers–Kronig relations:

$$\chi'_\rho(\omega) = \frac{1}{\pi} \int_{-\infty}^{\infty} \frac{d\tilde{\omega}}{\tilde{\omega} - \omega} \chi''_\rho(\tilde{\omega}). \quad (17)$$

So the net lineshift caused by the opening of the gap is given by

$$\Delta E = \int_0^{\infty} d\tilde{\omega} \frac{R_N(\tilde{\omega}) - R_G(\tilde{\omega})}{\tilde{\omega}}. \quad (18)$$

This is easily calculated for our model system:

$$\Delta E_{\text{model}} = \alpha \left\{ 2\epsilon \log 2 - \left( \frac{\epsilon}{\epsilon - \Delta} \right)^2 \left[ 2\epsilon \log \left( \frac{2\epsilon}{\epsilon + \Delta} \right) + 2\Delta \log \left( \frac{2\Delta}{\epsilon + \Delta} \right) \right] \right\}. \quad (19)$$

We plot this shift as a function of the gap in figure 3. It is a shift *away* from the power-law tail, i.e. towards lower binding energy.

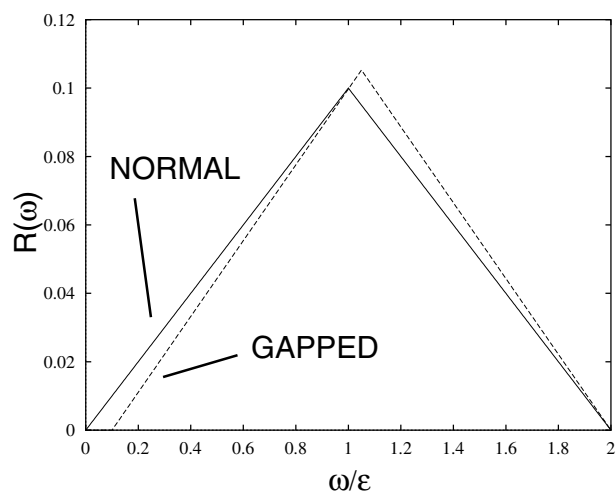


**Figure 2.**  $R(\omega)$  for the constant-density-of-states model, with and without a gap of  $\Delta/\epsilon = 0.05$ . The asymmetry exponent is  $\alpha = 0.1$ .

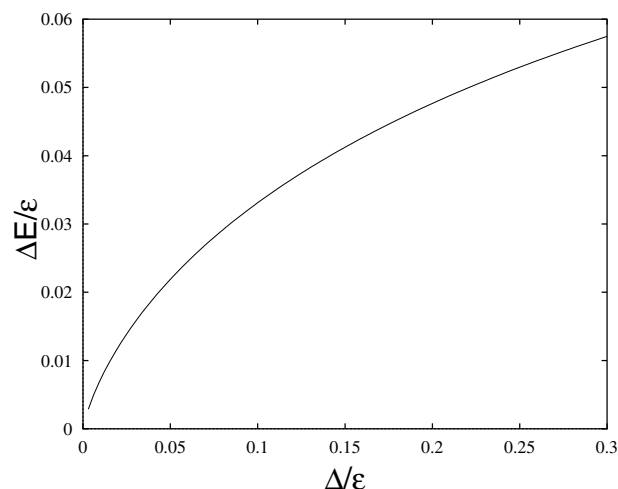


**Figure 3.** The overall lineshift for the flat-density-of-states model at various gap magnitudes. This is a shift away from the power-law tail, i.e. to lower binding energy. ( $\alpha = 0.1$ .)

A plot of the modified spectral function, convoluted with a Lorentzian to mimic the finite core lifetime, was shown in figure 1. While the coherent part of the spectral function (delta function) and its incoherent power-law tail have been mixed by the convolution into one smooth lineshape, this clearly demonstrates both of the effects discussed above—there is an overall shift on the line towards lower binding energy (to the right), and spectral weight is transferred from the tail of the line to the peak, making it seem sharper and more symmetric. It is this sharpening of the line which is the key signature of the failure of the orthogonality catastrophe.

While this model is obviously a gross oversimplification, it does illustrate the two main effects of opening a gap at the Fermi energy; to restate—the delta-function peak at threshold is partially restored, and there is an overall shift in the position of the lineshape towards lower binding energy.



#### 4. Superconducting systems

A similar analysis can be performed for a superconductor. The same basic physics holds as for the toy model considered above, but the density–density correlation function now factorizes into normal and anomalous parts, so we must consider

$$P(i\Omega_n) = \frac{1}{v^2} \sum_{p,k} |V(k, p)|^2 \frac{1}{\beta} \sum_{ip_n} [\mathcal{G}(p, ip_n) \mathcal{G}(k, ip_n + i\Omega_n) - \mathcal{F}(p, ip_n) \mathcal{F}^\dagger(k, ip_n + i\Omega_n)] \quad (20)$$

where  $i\Omega_n$  and  $ip_n$  are Matsubara frequencies.

Performing the frequency summation and continuing back to real frequencies yields the expression for  $R(\omega)$  in a superconductor. At zero temperature and for  $\omega > 0$  this reduces to

$$R(\omega) = \frac{1}{v^2} \sum_{k,p} |V(k, p)|^2 \left\{ \left( v_p^2 u_k^2 + \frac{\Delta_p \Delta_k}{4E_p E_k} \right) \delta(\omega - E_p - E_k) \right\} \quad (21)$$

where

$$u_k^2 = \frac{1}{2} \left( 1 + \frac{\xi_k}{E_k} \right) \quad v_k^2 = \frac{1}{2} \left( 1 - \frac{\xi_k}{E_k} \right)$$

are the coherence factors and  $E_k = \sqrt{\xi_k^2 + \Delta_k^2}$  is the excitation energy.

We now examine both s- and d-wave superconductors for two different single-particle energy dispersions, the linear dispersion of the previous section and a two-dimensional tight-binding model, and observe how the XPS lineshapes change upon the opening of the superconducting gap.

##### 4.1. Linear dispersion

As before, we assume a flat single-particle density of states of the form

$$N(\omega) = \begin{cases} N_0 & |\omega| < \epsilon \\ 0 & |\omega| > \epsilon. \end{cases} \quad (22)$$

In a BCS s-wave superconductor with a spherical Fermi surface in the normal state, the density of excitations is given by

$$N(E) = \begin{cases} N_0 \frac{E}{\sqrt{E^2 - \Delta_0^2}} & \text{if } E > \Delta_0 \\ 0 & \text{otherwise.} \end{cases} \quad (23)$$

Taking advantage of the delta function, an integral expression for the  $R(\omega)$  of an s-wave superconductor is obtained:

$$R_S(\omega) = \alpha \int_{\Delta}^{\omega - \Delta} \frac{E_p(\omega - E_p) + \Delta^2}{\sqrt{E_p^2 - \Delta^2} \sqrt{(\omega - E_p)^2 - \Delta^2}} dE_p. \quad (24)$$

We plot  $R_S(\omega)$  in figure 4. The finite value of  $R_S(\omega) = \pi \Delta$  at  $\omega = 2\Delta$  is a consequence of the divergent, but integrable, density of states for  $E \rightarrow \Delta$ . In the same manner as before we can calculate the lineshape (figure 5) and shift (figure 6) for an s-wave superconductor. The existence of the gap in a superconductor produces the same effects as it does in the band metal. Again there is a partial restoration of the delta-function peak, with a suppression of

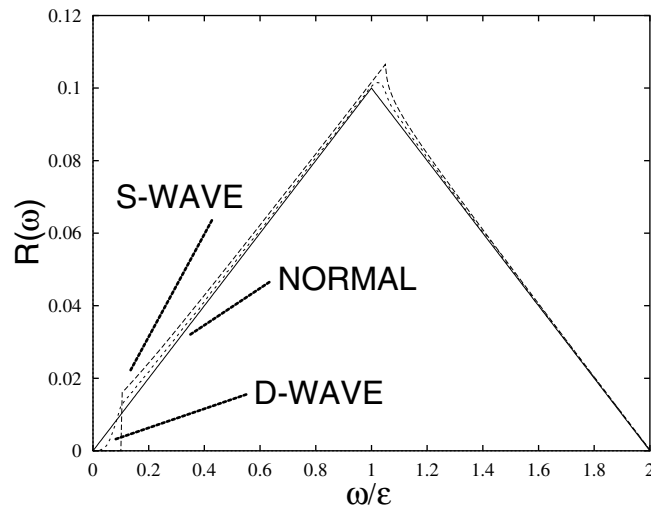


**Figure 4.**  $R(\omega)$  for a band metal in its normal state and for both s- and d-wave superconductors with a gap of  $\Delta/\epsilon = 0.05$ . ( $\alpha = 0.1$ .)

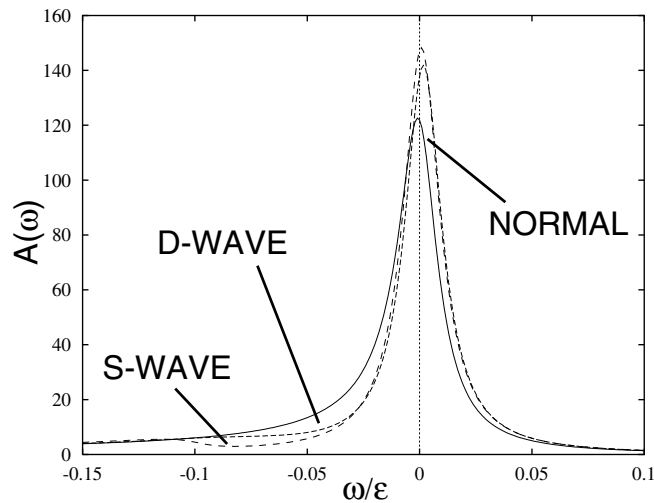


**Figure 5.** XPS lineshapes for the normal metal and s- and d-wave superconductors with a gap of  $\Delta/\epsilon = 0.05$ .  $1/\tau = 0.01\epsilon$  and  $\alpha = 0.1$ . As in the band metal, the superconductor lineshapes exhibit a delta-function restoration and an overall shift upon the opening of the gap.

the power-law tail for  $\omega < 2\Delta$ , and an overall shift of the line. These effects are however somewhat less pronounced than in the toy model.

The case of a d-wave superconductor, where gap nodes lead to the presence of low-energy excitations even for  $\Delta \neq 0$ , is subtly different. In this case the orthogonality catastrophe fails not because of the absence of zero-energy excitations, but because the number of zero-energy particle-hole pairs produced remains countable. More formally, the opening of a d-wave gap at zero temperature means that the leading term in  $R(\omega)$  is no longer  $\alpha\omega$  but now  $\beta\omega^3$ , and so the logarithm found from equation (9) in the case of a metal is eliminated. Unlike the s-wave case, the spectral function does have incoherent structure for  $0 < \omega < 2\Delta$ , but this

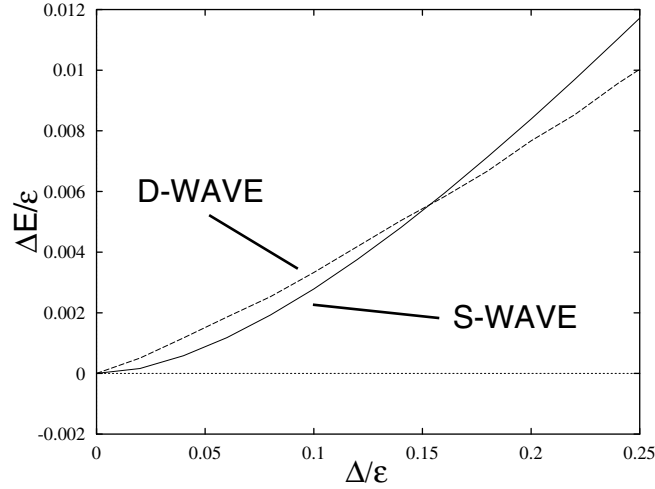


**Figure 6.** Magnitudes of overall lineshifts to lower binding energy for s- and d-wave superconductors assuming a linear single-particle dispersion and the asymmetry exponent  $\alpha = 0.1$ .

is accompanied by a slightly less pronounced transfer of spectral weight to a delta function at threshold.

The normal state has a circular Fermi surface, the superconducting two-dimensional d-wave gap being given by

$$\Delta_d(\phi) = \Delta_0 \cos(2\phi) \quad (25)$$

with  $0 \leq \phi \leq 2\pi$ . Both  $R(\omega)$  and the lineshift were obtained numerically via Monte Carlo integration. The lineshape was calculated as above.

The d-wave lineshape is shown along with that of the s-wave superconductor in figure 5 and the shift in figure 6. The presence of nodes in the gap leads to a slightly different gap dependence of the shift in the core line; in fact the d-wave lineshift is *larger* at small  $\Delta$  than in the s-wave case. The shifts can be fitted to power laws at small  $\delta = \Delta/\epsilon$ . The shift for the s-wave superconductor is given by  $\Delta E_s = 1.11\alpha\delta^{1.60}$  and the d-wave shift by  $\Delta E_d = 0.51\alpha\delta^{1.18}$  with an uncertainty of  $\pm 0.01$  in both the coefficient and the power.

If we assume that the gap opens as  $\sqrt{\eta}$  (where  $\eta = (T_c - T)/T_c$ ), as would be expected of a mean-field order parameter for  $T \approx T_c$ , this translates into a shift in the line scaling as  $\Delta E_s \sim \eta^{0.8}$  in the s-wave case and  $\Delta E_d \sim \eta^{0.25}$  in the d-wave case.

#### 4.2. Tight-binding model

In order to make closer contact with real high- $T_c$  superconductors, we also evaluated lineshapes and shifts for a d-wave superconductor on a half-filled square lattice with underlying tight-binding electron dispersion

$$\epsilon(k_x, k_y) = -2t(\cos k_x + \cos k_y) - 4t' \cos k_x \cos k_y \quad (26)$$

where  $t$  is the nearest-neighbour and  $t'$  the next-nearest-neighbour hopping integral. We chose  $t'/t = -0.35$  as being representative of the in-plane Cu d band in a ‘standard’ 123 compound such as  $\text{YBa}_2\text{Cu}_3\text{O}_{7-\delta}$ . A ‘standard’ 2212 compound such as  $\text{Bi}_2\text{Sr}_2\text{CaCu}_2\text{O}_{8+x}$  would have  $t'/t = -0.2$  [14] but this will not change our results significantly.

We model a superconductor with d-wave symmetry on a square lattice with a gap function of the form

$$\Delta_d(k_x, k_y) = \frac{\Delta_0}{2}(\cos(k_x) - \cos(k_y)). \quad (27)$$

The results for  $R(\omega)$  for this model of the normal and superconducting state are shown in figure 7. Once again we have set the coefficient of the leading linear term in the tight-binding metal to be 0.1, so the XPS asymmetry exponent for the system without a gap is  $\alpha = 0.1$ . For comparison with our previous models we consider a gap size of  $\Delta_0 = 0.05(4|t|)$ . In general,  $t$  is of the order of 0.25 eV. This gives  $\Delta_0 = 50$  meV which is clearly larger than in the real compounds, but not unreasonably so; estimates for YBCO yield  $\Delta_0 \approx 16$  meV and for BSSCO  $\Delta_0 \approx 30$  meV [15].

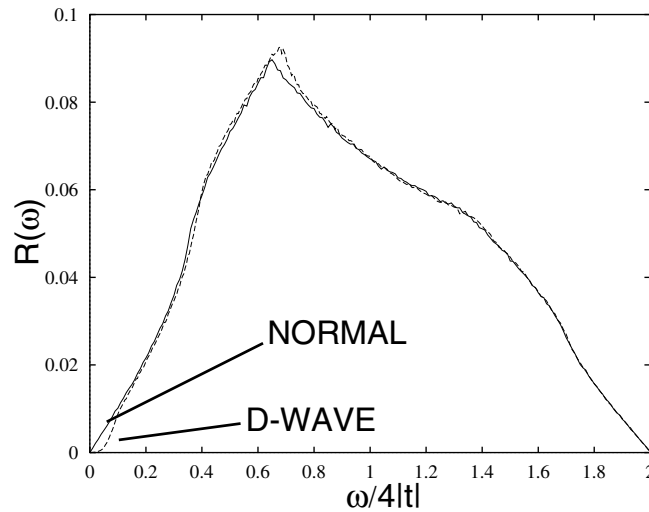


**Figure 7.**  $R(\omega)$  for tight-binding metal with  $t'/t = -0.35$  in the normal state and in a d-wave superconducting state with  $\Delta_0/4|t| = 0.05$ . Once again,  $\alpha = 0.1$ .

The resulting lineshapes and shifts for these coefficients are displayed in figures 8 and 9. Clearly the overall trends are exactly the same as those found in the more general models; a sharpening of the XPS line and a shift to lower binding energy, but both trends are somewhat more marked than in the constant-density-of-states model with the same parameters (cf. figures 5 and 6), and the shift is now very nearly linear in  $\Delta_0$ .

The size of shift which we find may be something of an underestimate of the true shift in the cuprates, since we neglect all corrections to screening of the core hole which arise from electron–electron interaction, which is known to be strong in these systems. An improved estimate might be found by incorporating a Hubbard  $U$ -term in the model, and evaluating a random-phase-approximation series for the screened susceptibility. Such a procedure has proved necessary to obtain quantitative estimates of the local spin susceptibility in these systems [17]. Screening through electron–electron interaction is of course a dynamical process, and leads to corrections to the lineshape and gap dependence of the shift, as well as to its overall scale. These effects do *not* change the underlying physics, can in principle be included in our calculation scheme, and may need to be included in any serious quantitative attempt to fit experimental lineshapes and lineshifts. We note also that attempts to fit the modified asymmetric lineshape found in the presence of a gap using a standard Doniach–Sunjic lineshape can lead to artificially low values of  $\alpha$ .

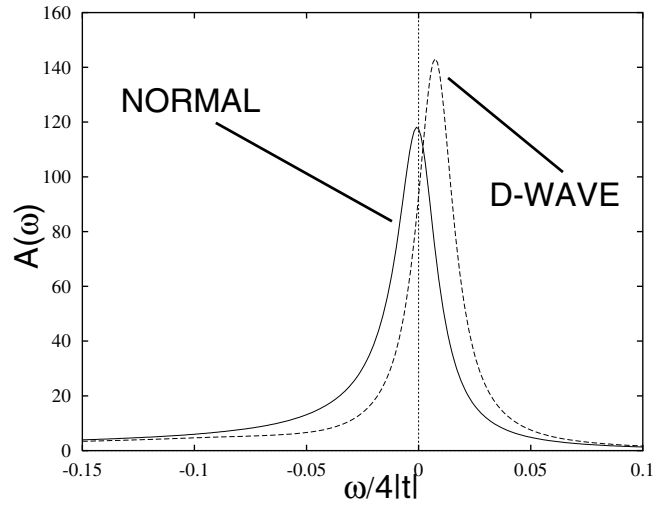


**Figure 8.** XPS lineshapes for a tight-binding metal in the normal state and in a d-wave superconducting state.  $\Delta_0/4|t| = 0.05$ ,  $1/\tau = 0.01|4t|$ , and  $\alpha = 0.1$ .

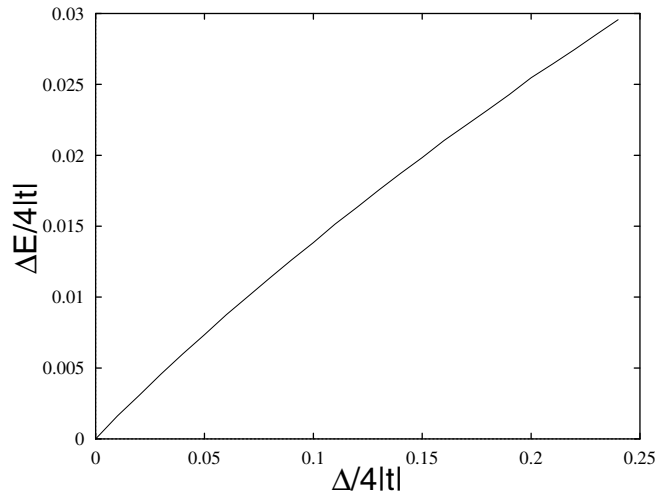


**Figure 9.** Overall lineshifts to lower binding energy for a d-wave superconductor with a tight-binding dispersion in the normal state as a function of the gap parameter  $\Delta_0/4|t|$ . Once again,  $\alpha = 0.1$ .

## 5. Pseudogaps and comparison with experiment

Pseudogap behaviour, which can be loosely defined as the (partial) loss of low-energy excitations without the emergence of order, has been observed in many strongly correlated electron systems<sup>1</sup>. The best known example is provided by the underdoped cuprate superconductors, where evidence for the opening of a pseudogap is found from NMR [1] and ARPES experiments at temperatures between some high-energy scale  $T^*$  and the superconducting transition

<sup>1</sup> This rule of thumb leads to some confusion of terms in cases where a true gap opens in the absence of long-range order, for example in the one-dimensional Hubbard model at half-filling.

temperature  $T_c$ . As a function of doping,  $T^*$  interpolates between the Néel temperature  $T_N \sim 800$  K of the undoped Mott insulator and the transition temperature  $T_c \sim 100$  K of the optimally doped superconductor.

What could XPS teach us about the opening of a pseudogap in this case? If the pseudogap seen in the NMR is a precursor to the formation of superconducting order at low temperatures, coming about, for example, through the formation of ‘incoherent’ pairs of electrons, then its effects on XPS lines will be broadly the same as those for a true gap. If on the other hand the pseudogap is not a precursor to superconductivity but, as has been suggested, a gap for spin excitations only, then XPS spectra would undergo little or no change at  $T^*$ . In this way the characteristic XPS signatures of gap opening—the sharpening of an asymmetric core line and/or a shift of lines to lower binding energy—could be used to distinguish between different theories of pseudogapped systems.

A shift in core lines to lower binding energy *has* been reported for XPS spectra taken above and below  $T_c$ , and for spectra taken above and below  $T^*$  in the cuprate high-temperature superconductor  $\text{Bi}_2\text{Sr}_2\text{Ca}_{1-x}\text{Y}_x\text{Cu}_2\text{O}_{8+\delta}$  [16]. At first sight this seems to offer confirmation of exactly the type of effect which we predict on the basis of core-hole screening—namely that the opening of a gap for joint spin *and charge* excitations modifies the XPS lineshape. However, the quoted experimental values of the shift are of order 100 meV for lines with an asymmetry  $\alpha = 0.04$ . This is much larger than can be reconciled with our simple model; using the tight-binding model considered above, together with the parametrization  $\alpha = 0.04$  and  $\Delta_0 = 30$  meV, we would anticipate a shift in the XPS line of order 1.2 meV. Individual features in XPS spectra can currently be resolved on a scale of meV, so allowing for a probable underestimation of  $\alpha$ ; our prediction for the shift is in principle observable, but only at the lower limit of what can be measured. Charge-density-wave systems which are better conductors in the metallic state and have gaps of order 100 meV are therefore probably better candidates for testing these ideas.

In fact no very strong conclusion can be drawn from the disagreement between our estimate and the reported shift in line for  $\text{Bi}_2\text{Sr}_2\text{Ca}_{1-x}\text{Y}_x\text{Cu}_2\text{O}_{8+\delta}$ , because analysing the metal–superconductor transition in such a strongly correlated system in terms of the tight-binding model and BCS models cannot always be expected to give reliable answers, especially in the underdoped ‘pseudogap’ regime. Nevertheless we believe that our calculation provides the correct starting point for understanding such experiments, and explanations for the observed lineshift other than the suppression of screening of the core hole by the opening of the gap should therefore be considered.

## 6. Conclusions

The gross effects seen in XPS lineshapes for metallic systems when a gap opens are very robust and independent of the choice of model. The core line undergoes an overall shift to lower binding energy and spectral weight is transferred from the power-law tail of the line to its peak, leading to a sharpening of the line and some loss of overall asymmetry. Modifications to the lineshape are more easily seen in systems where the gap is large compared with the intrinsic width of the core level. In this limit subtle differences can also be seen between different models, although we note that these differences may be quite difficult to detect in practice.

Any analysis of gap structure should involve several complementary methods. Angle-resolved photoemission (ARPES) has the ability to provide high-resolution information about the momentum dependence of the density of states with little degradation due to lifetime

effects. As such, ARPES has been extensively used for the exploration of gapped and pseudo-gapped systems, most notably in the cuprate superconductors [18]. However, ARPES has the disadvantage of probing both the spin and charge channels simultaneously. Independent information about either of these channels must come from some other source.

In this arena, XPS shows great promise. Lifetime broadening is at first sight problematic, but in cases where sufficiently narrow core lines can be found, XPS offers a potentially rich source of information about the changes taking place when a gap opens in the charge channel of a many-electron system. This may be particularly useful when taken in conjunction with NMR experiments [3].

For XPS lineshapes with both high resolution and high statistics, deconvolution of the lineshape can remove much of the lifetime broadening. We have applied code written to remove Lorentzian lifetime broadening from x-ray absorption (XAS) spectra [19] successfully to both real and simulated core-level XPS spectra, and find that where the (statistical) noise in spectra is sufficiently small, lifetime broadening can be reduced to levels where the changes in lineshape associated with the opening of a gap of 10–100 meV can be observed. The effort involved in measuring XPS spectra with sufficient accuracy should also be weighed against the need for background subtraction in ARPES, and the time required to measure the entire Fermi surface. Since with XPS there is only one spectrum to measure for each temperature, measuring spectra for many different temperatures spanning a phase transition to study the evolution of lineshapes is also feasible.

For simplicity, we have chosen to work within perturbation theory and to discuss only models which have simple non-interacting quasiparticle excitations. Both of these restrictions can be relaxed, and many of the same physical considerations apply to core levels coupled to strongly interacting electron systems. Experimentally it might well be interesting to look at the effect on XPS lines of metal–insulator or charge-density-wave transitions where the intrinsic gap scale is very much larger ( $\sim 10^2$  meV), and the effects of gap opening can be expected to be more pronounced.

## Acknowledgments

We are grateful to the authors of [19] for making their deconvolution code available to us, and are pleased to acknowledge many helpful conversations with Jim Allen, Franz Himpsel, and Robert Joynt. This work was supported under the grant DMR-9704972 .

## References

- [1] Imai T *et al* 1993 *Phys. Rev. Lett.* **70** 1002  
Howes A P *et al* 1992 *Physica C* **193** 189
- [2] Shannon N and Joynt R 2000 *Solid State Commun.* **115** 441
- [3] Shannon N 2000 *J. Phys.: Condens. Matter* **12** 7045
- [4] Doniach S and Sunjic M 1970 *J. Phys. C: Solid State Phys.* **3** 285
- [5] Wertheim G K and Citrin P H 1978 *Photoemission in Solids I* (Berlin: Springer)
- [6] Mizokawa T *et al* 1998 *Phys. Rev. B* **57** 9550
- [7] Combescot M and Nozières P 1971 *J. Physique* **32** 913
- [8] Mahan G D 1990 *Many Particle Physics* (New York: Plenum) p 178
- [9] Langreth D C 1972 *Phys. Rev. B* **1** 471
- [10] Anderson P W 1967 *Phys. Rev. Lett.* **18** 1049
- [11] Hopfield J J 1969 *Comment. Solid State Phys.* **2** 40  
See also  
Hopfield J J 1962 *Proc. Int. Conf. on the Physics of Semiconductors (Exeter, 1962)* (Bristol: Institute of Physics Publishing) p 75

- 
- [12] Ohtaka K and Tanabe Y 1990 *Rev. Mod. Phys.* **62** 929  
For a recent pedagogical overview see also  
Gogolin A, Nersisyan A and Tsvelik A 1998 *Bosonization of Strongly Correlated Electron Systems* (Cambridge:  
Cambridge University Press)
- [13] Nozières P and de Dominicis C T 1969 *Phys. Rev.* **178** 1097
- [14] Koltentbah B and Joynt R 1997 *Rep. Prog. Phys.* **60** 23
- [15] Shen Z X and Dessau D S 1995 *Phys. Rep.* **253** 1
- [16] Tjernberg O *et al* 1997 *Phys. Rev. Lett.* **79** 499
- [17] Joynt R and Li Q P 1992 *Phys. Rev. B* **47** 530
- [18] See e.g.,  
Ding H *et al* 1996 *Nature* **382** 51  
Loeser A G *et al* 1996 *Science* **273** 325  
See also discussion in  
Lynch D W and Olson C G 1999 *Photoemission Studies of High-Temperature Superconductors* (Cambridge:  
Cambridge University Press)
- [19] Loeffen P W *et al* 1996 *Phys. Rev. B* **54** 14 877